PERGAMON

International Journal of Solids and Structures 39 (2002) 311–324

INTERNATIONAL JOURNAL OF SOLIDS and STRUCTURES

www.elsevier.com/locate/ijsolstr

Micromechanical bounds for the effective elastic moduli of granular materials

N.P. Kruyt [a,*], L. Rothenburg [b]

[a] *Department of Mechanical Engineering, University of Twente, P.O. Box 217, 7500 AE Enschede, Netherlands*
[b] *Department of Civil Engineering, University of Waterloo, Waterloo, Ont., Canada N2L 3G1*

Received 26 April 2001

Abstract

This study deals with bounds for the effective elastic moduli of granular materials in terms of micromechanical parameters. The case considered is that of two-dimensional isotropic assemblies of non-rotating particles with bonded contacts and a linear elastic contact constitutive relation. Based on variational principles, rigorous upper and lower bounds are obtained for the elastic moduli. To this end, compatible and equilibrated fields are constructed from local characteristics, based on approximate equilibrium and compatibility, respectively. Results of discrete element simulations are used to compare the obtained bounds with the actual moduli. This comparison shows that the actual moduli are narrowly bracketed by these bounds. The corresponding fields of relative displacement and force at the contacts are analysed, showing fairly close agreement with those obtained from the discrete element simulations.

Keywords: Granular materials; Micromechanics; Elasticity; Variational principles; Bounds

1. Introduction

In many industrial, geotechnical and geophysical applications dealing with granular materials, knowledge of the mechanical behaviour of granular materials is important. This knowledge is expressed by a constitutive relation, which usually is based on continuum mechanics, and involves heuristic assumptions. Contrary to this approach is the micromechanical approach, in which a granular material is modelled as an assembly of particles that interact at *contacts*. The micromechanical approach therefore incorporates the discrete nature of granular materials. An objective of this approach is to derive macroscopic characteristics from microscopic characteristics, such as contact geometry and contact constitutive relation.

The relatively simple case that is considered here is that of the effective elastic behaviour of two-dimensional assemblies of non-rotating particles with bonded contacts. It is expected that many salient features of this simple system will hold, at least qualitatively, for more complicated systems. Some

* Corresponding author. Tel.: +31-53-4892528; fax: +31-53-4893695.
E-mail addresses: n.p.kruyt@wb.utwente.nl (N.P. Kruyt), leoroth@uwaterloo.ca (L. Rothenburg).

0020-7683/01/$ - see front matter
PII: S0020-7683(01)00200-1

applications of the current model are the initial elastic deformation of dense or cemented granular materials and certain fibrous media.

The outline of this paper is as follows. In Section 2 some micromechanical quantities and the contact constitutive relation that is considered here are described. Then minimum potential energy and minimum complementary energy principles are recapitulated in Section 3 that were derived by Kruyt and Rothenburg (1998). To use these principles to obtain rigorous bounds for the moduli, compatible fields for the relative displacements at the contacts and equilibrated fields for the forces at the contacts must be constructed. The construction of compatible fields is fairly trivial, while a general construction of equilibrated fields of contact forces (Satake, 1992) is described in Section 4. In Section 5, a compatible field that is close to force equilibrium is determined based on local analyses, which in turn gives an upper bound for the moduli. Similarly, based on local analyses, an equilibrated field that is close to compatibility is determined, which yields a lower bound for the moduli. In Section 6 the results of discrete element simulations (Cundall and Strack, 1979) are used to compare the obtained bounds with the actual moduli, and to analyse the approximate fields for the relative displacements and forces at the contacts. Finally, findings from this study are discussed.

The usual sign convention from continuum mechanics is employed for stress and strain, according to which tensile stresses and strains are considered positive. The summation convention is adopted, implying a summation over repeated subscripts.

2. Micromechanics

Branch vectors l_i^{pq} are defined as the vectors that connect the centres of particles p and q that are in contact. These branch vectors form closed loops, or polygons, as depicted in Fig. 1. For future reference the *polygon vector* h_j^{RS} (Rothenburg, 1980; Kruyt and Rothenburg, 1996) is also defined in Fig. 1: it is the vector that is obtained by counter-clockwise rotation over 90° of the *rotated polygon vector* g_i^{RS} that connects the centres of adjacent polygons R and S.

Contacts can be identified in two ways: by the particles involved, or by the polygons involved. The first way will be indicated by using lower case superscripts, while the second way will be indicated by upper case superscripts. The adopted convention for the equivalence of contact RS with contact pq is that the vectors g_i^{RS} and l_i^{pq} form a right-handed system. For example, in Fig. 1 contact RS (and not SR) is equivalent to contact pq.

An important statistical measure of the contact geometry is *coordination number* Γ, that is the average number of contacts per particle. It is a measure of the solid fraction η: for isotropic assemblies the relation $\eta \cong (\pi/\Gamma)/\tan(\pi/\Gamma)$ was derived by Kruyt and Rothenburg (1996).

In the absence of body forces the quasi-static force equilibrium conditions for particle p are

$$\sum_q f_i^{pq} + f_i^{p\beta} = 0, \tag{1}$$

where the summation is over the particles q that are in contact with particle p and $f_i^{p\beta}$ is the force exerted by the boundary on particle p (if present). The term is $f_i^{p\beta}$ only present for the "boundary particles" that are hatched in Fig. 1.

The kinematic analogue of the equilibrium conditions is formed by the compatibility conditions for the relative displacements between particle centres. The relative displacement Δ_i^{pq} between particles p and q is defined by

$$\Delta_i^{pq} = U_i^q - U_i^p, \tag{2}$$

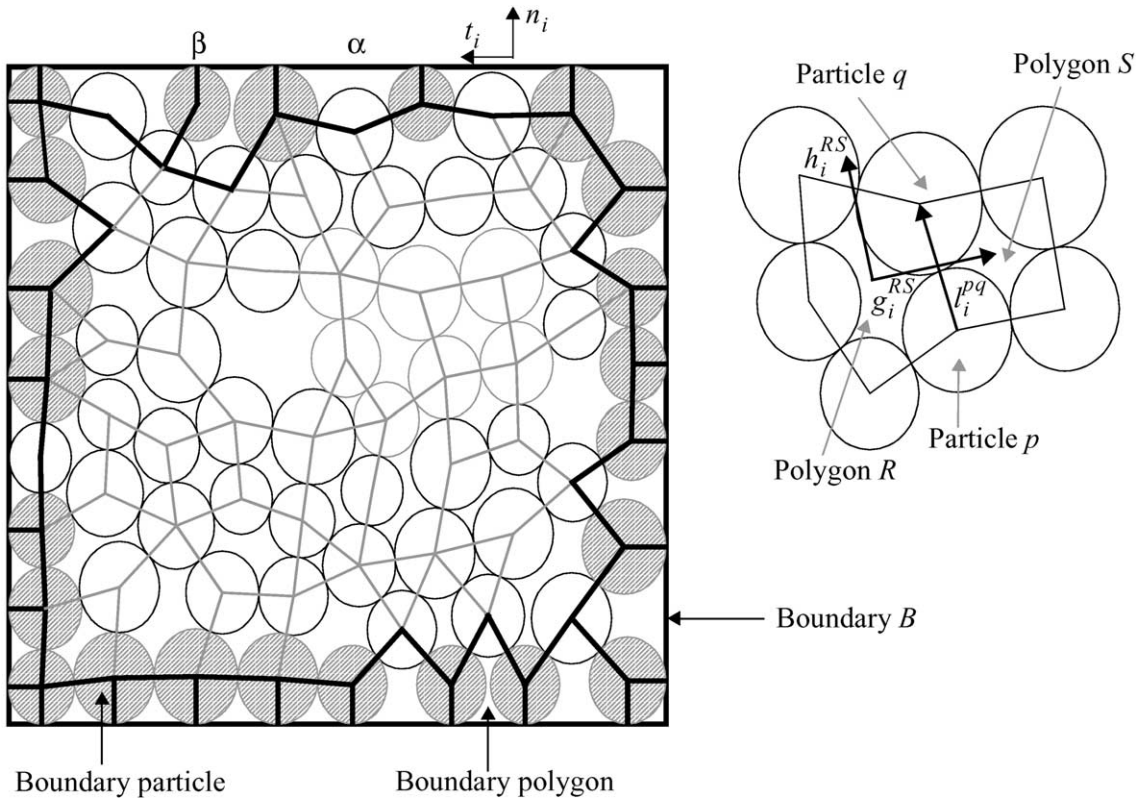

Fig. 1. Polygons, branch vector, polygon vector and rotated polygon vector.

where U_i^p is the displacement of the centre of particle p. The compatibility equations are (Rothenburg, 1980; Kruyt and Rothenburg, 1996)

$$\sum_S \Delta_i^{RS} + \Delta_i^{R\alpha} = 0, \tag{3}$$

where the summation is over the sides S that form polygon R and $\Delta_i^{R\alpha}$ is the relative displacement corresponding to a boundary link of polygon R (if present). The term $\Delta_i^{R\alpha}$ is only present for the "boundary polygons" that are completely enclosed by thick black lines in Fig. 1.

2.1. Contact constitutive relation

The case considered is the relatively simple case of the linear elastic behaviour of bonded assemblies of *non-rotating* particles. The contact geometry is shown in Fig. 2, showing the unit normal and tangential vectors n_i^{pq} and t_i^{pq} at the contact. At the contact two linear springs are present in normal and tangential directions with corresponding stiffnesses k_n and k_t. The constitutive relation at the contact is

$$f_\mathrm{n}^c = k_\mathrm{n}\Delta_\mathrm{n}^c, \qquad f_\mathrm{t}^c = k_\mathrm{t}\Delta_\mathrm{t}^c, \tag{4}$$

where f_n^c and f_t^c are the normal and tangential components of the contact force, while Δ_n^c and Δ_t^c are the normal and tangential components of the relative displacement at the contact. The *stiffness ratio* is defined by $\lambda = k_\mathrm{t}/k_\mathrm{n}$.

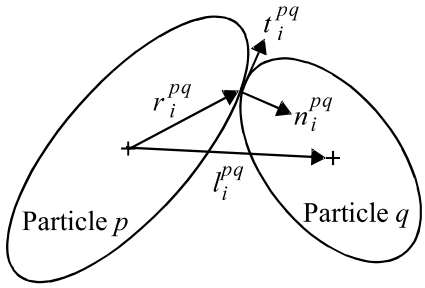

Fig. 2. Contact geometry of two particles that are in contact.

The contact constitutive relation can also be expressed by stiffness matrix S_{ij}^c or a compliance matrix C_{ij}^c

$$\begin{aligned} f_i^c &= S_{ij}^c \Delta_j^c, \quad S_{ij}^c = k_\mathrm{n} n_i^c n_j^c + k_\mathrm{t} t_i^c t_j^c, \\ \Delta_i^c &= C_{ij}^c f_j^c, \quad C_{ij}^c = \tfrac{1}{k_\mathrm{n}} n_i^c n_j^c + \tfrac{1}{k_\mathrm{t}} t_i^c t_j^c. \end{aligned} \tag{5}$$

In the next subsection it will be shown that the cases with and without particle rotation constitute two limit cases of a more complex constitutive relation.

2.2. Effect of rotation

To clarify the relation between the cases of rotating and non-rotating particles, a more complex contact constitutive relation is considered where *contact couples* are also included, besides the moment due to the contact force (see also Chang and Liao, 1990; Oda and Iwashita, 2000). Note that this contact constitutive relation is only considered in this subsection.

The rotation of particle p is denoted by ω^p. Including particle rotation, the relative displacement δ_i^{pq} *at the contact* between particles p and q is given by $\delta_i^{pq} = [U_i^q + e_{ji} r_j^{qp} \omega^q] - [U_i^p + e_{ji} r_j^{pq} \omega^p]$, where e_{ij} is the two-dimensional permutation tensor and r_i^{pq} is the vector from the centre of particle p to the contact point between particles p and q (see also Fig. 2). The linear elastic contact constitutive relation for force f_i^{pq} and couple κ^{pq} is

$$f_i^{pq} = S_{ij}^{pq} \delta_j^{pq}, \qquad \kappa^{pq} = k_\omega (\omega^q - \omega^p), \tag{6}$$

where S_{ij}^{pq} is identical to that in Eq. (5) and k_ω is a couple stiffness.

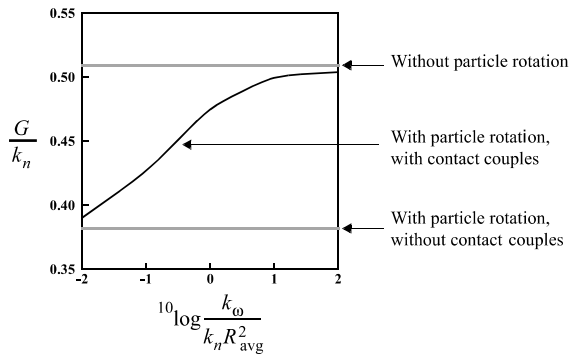

Fig. 3. Effect of couple stiffness k_ω on effective shear modulus G as computed from discrete element simulations. The results are for coordination number $\Gamma = 4.0$ and stiffness ratio $\lambda = 1.0$. Here R_{avg} denotes the average particle radius.

Discrete element simulations with bonded contacts were performed for this case which includes particle rotation, and the effect on the effective shear modulus of varying the couple stiffness k_ω was studied at constant normal and tangential stiffnesses. The result in Fig. 3 shows that the case of rotating particles without contact couples (trivially) corresponds to $k_\omega \to 0$, while the case of non-rotating particles corresponds to $k_\omega \to \infty$.

3. Variational principles

Two variational principles were derived by Kruyt and Rothenburg (1998) for assemblies of non-rotating particles with the linear elastic contact constitutive relation (4). These principles are discrete analogues of the classical minimum potential energy and minimum complementary energy principles in continuum elasticity (see for example Washizu, 1968).

3.1. Minimum potential energy principle

Two relative displacement fields $\{\Delta_i^c\}$ and $\{\Delta_i^{*c}\}$ are considered that satisfy the compatibility conditions (3) and are consistent with displacements at the boundary B that correspond to uniform strain along the boundary. The associated force fields are $\{f_i^c\}$ and $\{f_i^{*c}\}$. The force field $\{f_i^c\}$ satisfies the equilibrium conditions (1), contrary to the force field $\{f_i^{c*}\}$. Then the minimum potential energy principle is

$$\frac{1}{2}\sigma_{ij}\varepsilon_{ij} = \frac{1}{2}\sum_{c\in S}\Delta_i^c f_i^c \leqslant \frac{1}{2}\sum_{c\in S}\Delta_i^{*c} f_i^{*c} \tag{7}$$

with equality if and only if $\Delta_i^{*c} \equiv \Delta_i^c$.

With prescribed strain, an upper bound for the moduli is obtained by evaluating the energy corresponding to a relative displacement field $\{\Delta_i^{*c}\}$.

3.2. Minimum complementary energy principle

Two force fields $\{f_i^c\}$ and $\{f_i^{*c}\}$ are considered that satisfy the equilibrium conditions (1) and are consistent with forces at the boundary B that correspond to uniform stress along the boundary. The associated relative displacement fields are $\{\Delta_i^c\}$ and $\{\Delta_i^{*c}\}$. The relative displacement field $\{\Delta_i^c\}$ satisfies the compatibility conditions (3), contrary to the relative displacement field $\{\Delta_i^{*c}\}$. Then the minimum complementary energy principle is

$$\frac{1}{2}\sum_{c\in S} f_i^{*c}\Delta_i^{*c} \geqslant \frac{1}{2}\sum_{c\in S} f_i^c\Delta_i^c = \frac{1}{2}\sigma_{ij}\varepsilon_{ij} \tag{8}$$

with equality if and only if $f_i^{*c} \equiv f_i^c$.

With prescribed stress, a lower bound for the moduli is obtained by evaluating the energy corresponding to a force field $\{f_i^{*c}\}$.

3.3. Uniform strain and uniform stress

Kruyt and Rothenburg (1998) used the minimum potential energy principle (7) to derive an upper bound for the moduli based on the *uniform strain assumption*

$$\Delta_i^{*c} = \varepsilon_{ij} l_j^c, \tag{9}$$

where l_j^c is the branch vector defined in Section 2.

The minimum complementary energy principle (8) was used to derive a lower bound for the moduli based on the *uniform stress assumption*

$$f_i^{*c} = \sigma_{ij} h_j^c, \tag{10}$$

where h_j^c is the polygon vector defined in Section 2.

4. Compatible and equilibrated solutions

To use these variational principles, general expressions for compatible relative displacement fields and equilibrated force fields must be constructed. The first is trivial, while the second is more involved. Both will be discussed here to show the analogy between the two approaches.

4.1. Compatible solutions

The full family of compatible solutions is obtained when the relative displacement field $\{\Delta_i^c\}$ is derived from a particle displacement field U_i^p according to Eq. (2). It is easily verified that this form satisfies the compatibility equations (3).

Prescribed boundary displacements determine the displacement of the boundary particles (see Fig. 1).

4.2. Equilibrated solutions

In the absence of body forces the full family of equilibrated solutions, as given by Satake (1992), will be recapitulated here. This method shows analogies with the method of mesh currents in electrical network theory (see for example Murdoch, 1970) and the Airy stress function in two-dimensional elasticity (see for example Washizu, 1968). The analogy with the Airy stress function will be shown in detail in Section 4.2.1.

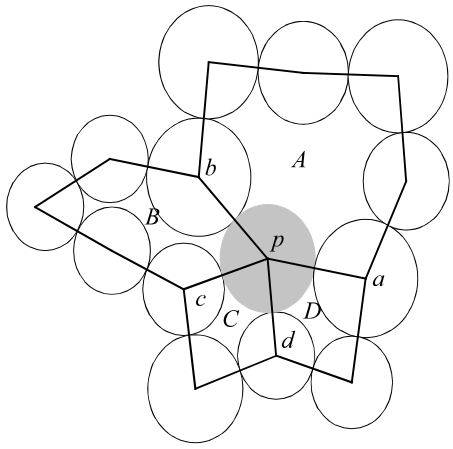

$$\sum_q f_i^{pq} = f_i^{pa} + f_i^{pb} + f_i^{pc} + f_i^{pd}$$

$$= [\Phi_i^D - \Phi_i^A] + [\Phi_i^A - \Phi_i^B] + [\Phi_i^B - \Phi_i^C] + [\Phi_i^C - \Phi_i^D] = 0$$

Fig. 4. Construction of equilibrated contact forces using force potentials.

A vector quantity Φ_i^R, the *force potential*, is associated with each polygon. The force f_i^{RS} at the contact corresponding to polygons R and S is then defined by

$$f_i^{RS} = \Phi_i^S - \Phi_i^R. \tag{11}$$

It is easily verified that this construction of contact forces leads to equilibrium for *all* particles. An example is shown in Fig. 4. Note further that this form satisfies Newton's third law

$$f_i^{qp} \equiv f_i^{SR} = \Phi_i^R - \Phi_i^S = -f_i^{RS} \equiv -f_i^{pq}. \tag{12}$$

Unlike their kinematic equivalents the particle displacements U_i^p, these force potentials Φ_i^R do not have a direct physical meaning.

The force potentials of the boundary polygons (see Fig. 1) are determined from prescribed forces at the boundary by assigning an arbitrary value to the force potential of an initial boundary polygon and using Eq. (11) to compute the force potential of subsequent polygons along the boundary.

4.2.1. Relation with the Airy stress function

Here the analogy between the construction with force potentials and the Airy stress function in two-dimensional elasticity will be shown. First a correspondence between the stress tensor σ_{ij} and a continuous force potential field is postulated

$$\sigma_{ij} = -e_{jk}\frac{\partial \Phi_i}{\partial x_k} \quad \text{or} \quad \begin{array}{ll} \sigma_{11} = -\frac{\partial \Phi_1}{\partial x_2} & \sigma_{12} = -\frac{\partial \Phi_1}{\partial x_1} \\ \sigma_{21} = -\frac{\partial \Phi_2}{\partial x_2} & \sigma_{22} = -\frac{\partial \Phi_2}{\partial x_1}. \end{array} \tag{13}$$

It is easily verified that this definition satisfies the quasi-static (continuum) equilibrium conditions without body forces $\partial \sigma_{ij}/\partial x_j = 0$.

Now it will be shown that the expression (13) is consistent with an expression for the average stress $\bar{\sigma}_{ij}$ in terms of boundary forces. The area of the region of interest is S and its boundary is B. The average stress is given by $\bar{\sigma}_{ij} = (1/S)\sum_{\beta \in B} f_i^\beta x_j^\beta$, see for example Kruyt and Rothenburg (1996). From Eq. (13) and Gauss' theorem it follows

$$S\bar{\sigma}_{ij} = \int_S \sigma_{ij}\,\mathrm{d}S = -e_{jk}\int_S \frac{\partial \Phi_i}{\partial x_k}\,\mathrm{d}S = -e_{jk}\int_B \Phi_i n_k\,\mathrm{d}S, \tag{14}$$

where n_i is the normal vector at the boundary with associated tangential vector t_i (see also Fig. 1). By noting that $-e_{jk}n_k = t_j = \mathrm{d}x_j/\mathrm{d}s$ and performing a partial integration along the closed boundary B, this can be rewritten as

$$S\bar{\sigma}_{ij} = \int_B \Phi_i \frac{\mathrm{d}x_j}{\mathrm{d}s}\,\mathrm{d}s = -\int_B \frac{\mathrm{d}\Phi_i}{\mathrm{d}s} x_j\,\mathrm{d}s = \sum_\beta f_i^\beta x_j^\beta, \tag{15}$$

where the final equality follows after some algebra from the assumption of point loading, the definition of contact force in terms of force potentials (11) and the adopted convention from Section 2 for the equivalence of contact RS with contact pq.

Finally, the relation with the Airy stress function χ is established by the definitions

$$\Phi_1 = -\frac{\partial \chi}{\partial x_2}, \qquad \Phi_2 = \frac{\partial \chi}{\partial x_1}. \tag{16}$$

Note that the usual definitions of the stress components in terms of second derivatives of the Airy stress function χ are retrieved

$$\sigma_{11} = \frac{\partial^2 \chi}{\partial x_2^2}, \quad \sigma_{12} = \sigma_{21} = -\frac{\partial^2 \chi}{\partial x_1 \partial x_2}, \quad \sigma_{22} = \frac{\partial^2 \chi}{\partial x_1^2}. \tag{17}$$

From Eq. (13) it follows that the force potential field that corresponds to uniform stress is given by

$$\Phi_i(x_j) = -\sigma_{ij} e_{jk} x_k + \Phi_i^0, \tag{18}$$

where the arbitrary constant vector Φ_i^0 does not affect the value of the contact forces.

The derivation of the construction of equilibrated force fields differs from the exposition of Satake (1992) in the following points: (i) it is demonstrated simply and directly that this construction leads to equilibrium for *all particles*; (ii) it is explained how boundary conditions are incorporated; (iii) the compatibility conditions are defined directly and in a physical manner; (iv) the analogy with the Airy stress function is shown in detail.

5. Local adjustment fields

To obtain an upper bound for the moduli from the minimum potential energy principle (7), a compatible relative displacement field will be constructed which leads to *approximate* equilibrium. To obtain a lower bound for the moduli from the minimum complementary energy principle (8), an equilibrated force field will be constructed which leads to *approximate* compatibility. Both approaches involve a local adjustment to a uniform field that uses only information on neighbours (particles or polygons).

5.1. Compatible relative displacement field

Consider a single particle p whose displacement U_i^p will be determined by a *local* adjustment: assume that the displacements of the particles q with which it is in contact, move uniformly according to the prescribed boundary strain, while the particle itself exhibits a fluctuation u_i^p on this field

$$U_i^p = \varepsilon_{ij} X_j^p + u_i^p, \qquad U_i^q = \varepsilon_{ij} X_j^q. \tag{19}$$

The corresponding relative displacements at the contacts are given by

$$\Delta_i^{pq} = \varepsilon_{ij} l_j^{pq} - u_i^p. \tag{20}$$

For each particle p its fluctuation displacement u_i^p is determined by requiring static equilibrium (1), or equivalently minimising the local potential energy with the fluctuation displacement u_i^p as the only degree of freedom

$$\left\{ \sum_q S_{ij}^{pq} \right\} u_j^p = \sum_q S_{ij}^{pq} \varepsilon_{jk} l_k^{pq}. \tag{21}$$

Since the boundary displacements are kept the same (zero displacement fluctuation on the boundary) and the average strain $\bar{\varepsilon}_{ij}$ is determined by the boundary displacements, $\bar{\varepsilon}_{ij} = (1/S) \int_B u_i n_j \, \mathrm{d}s$ (see for example Kruyt and Rothenburg, 1996), the average strain corresponding to the displacement fluctuations $\{u_i^p\}$ is zero.

This procedure of computing an estimate of the particle displacement is performed sequentially for all particles. Note that these computations are *uncoupled*.

The computation of the individual displacements is based on the assumption that its neighbours q move uniformly according to the prescribed strain. Since this will not be the case exactly, due to the presence of fluctuations u_i^q, the proposed procedure does *not* result in equilibrium of all particles.

By setting all fluctuation displacements $u_i^p \equiv 0$, the *uniform strain* bound derived by Kruyt and Rothenburg (1998) is retrieved, see also Eq. (9).

5.2. Equilibrated force field

Consider a single polygon R whose force potential Φ_i^R is determined by a *local* adjustment: assume that the force potentials of the neighbouring polygons S conform *uniformly* to the prescribed boundary stress (as given by Eq. (18)), while the polygon itself exhibits a fluctuation Φ_i^R on this field

$$\Phi_i^R = -\sigma_{ij} e_{jk} X_k^R + \phi_i^R, \qquad \Phi_i^S = -\sigma_{ij} e_{jk} X_k^S. \tag{22}$$

The corresponding forces at the contacts are given by

$$f_i^{RS} = -\sigma_{ij} e_{jk} g_k^{RS} - \phi_i^R = \sigma_{ij} h_j^{RS} - \phi_i^R, \tag{23}$$

where the rotated polygon vector g_j^{RS} and the polygon vector h_j^{RS} are depicted in Fig. 1.

For each polygon R its fluctuation ϕ_i^R is determined by requiring compatibility (3), or equivalently minimising the local complementary energy with the fluctuation ϕ_i^R as the only degree of freedom

$$\left\{ \sum_S C_{ij}^{RS} \right\} \phi_j^R = \sum_S C_{ij}^{RS} \sigma_{jk} h_k^{RS}. \tag{24}$$

Since the boundary forces are kept the same (zero fluctuation of the force potential on the boundary) and the average stress is determined by the boundary force, $\bar{\sigma}_{ij} = (1/S) \sum_{\beta \in B} f_i^\beta x_j^\beta$ (see for example Kruyt and Rothenburg, 1996), the average stress corresponding to the force potential fluctuations $\{\phi_i^R\}$ is zero.

This procedure of computing an estimate of the force potentials is performed sequentially for all polygons. Note that these computations are *uncoupled*.

The computation of the individual force potentials is based on the assumption that its neighbours S conform uniformly to the prescribed stress. Since this will not be the case exactly, due to the presence of fluctuations ϕ_i^S, the proposed procedure does *not* result in compatibility of all polygons.

By setting all fluctuations $\phi_i^R \equiv 0$, the *uniform stress* bound derived by Kruyt and Rothenburg (1998) is retrieved, see also Eq. (10).

6. Comparison with discrete element simulations

Discrete element simulations, as proposed by Cundall and Strack (1979), were performed with large assemblies of 50,000 disks from a fairly wide lognormal particle size distribution for nine different isotropic assemblies with average coordination numbers Γ in the range 4–6, and for each average coordination number for nine different stiffness ratios λ in the range 0.05–1.0. Two loading paths are sufficient for isotropic assemblies, compressive and shearing loading. The simulations are fully described in Kruyt and Rothenburg (2001). The bulk and shear modulus are determined from

$$\begin{aligned} \sigma_{11} + \sigma_{22} &= 2K(\varepsilon_{11} + \varepsilon_{22}), \\ \sigma_{11} - \sigma_{22} &= 2G(\varepsilon_{11} - \varepsilon_{22}), \\ \sigma_{12} &= 2G\varepsilon_{12}. \end{aligned} \tag{25}$$

First the actual moduli will be compared with those obtained from the discrete element simulations. Then some characteristics of the local adjustment fields of the relative displacement and force at the contact will be compared with those obtained from the simulations.

Although the described method will be compared with results from simulations on assemblies of *disks*, the method is equally applicable to particles of different shapes.

6.1. Bounds for the moduli

The obtained upper and lower local adjustment bounds for the moduli, together with the uniform strain and stress bounds of Kruyt and Rothenburg (1998), are given in Fig. 5 for compressive and shearing loading for various coordination numbers Γ and stiffness ratios λ. These improved local adjustment bounds are much tighter than the uniform strain and stress bounds, especially for low coordination numbers and in shear for high coordination numbers.

6.2. Group averages for relative displacements and forces

The boundary conditions, prescribed displacements or forces, tend to impose a regular pattern on the relative displacement and force at the contacts, as can be expected from continuum mechanics. This pattern depends on the orientation of the contact normal. Therefore it is logical to group contacts with similar orientations, and to compute *group averages* for relative displacement and force at contacts (see for example Rothenburg, 1980; Bathurst and Rothenburg, 1988; Kruyt and Rothenburg, 2001).

The regular pattern that can be expected from continuum mechanics for the relative displacement and force at contacts can be expressed by generalized uniform strain and generalized uniform stress expressions

$$\Delta_i^c = \zeta \varepsilon_{ij} l_j^c, \qquad f_i^c = \xi \sigma_{ij} h_j^c, \tag{26}$$

where $\zeta = 1$ for uniform strain and $\xi = 1$ for uniform stress. Note that ζ and ξ give the non-dimensional amplitudes of relative displacements and forces, respectively.

The group averages, corresponding to the local adjustment fields and to the actual fields from the simulations, for relative displacement and force at the contacts were computed. They matched the expressions (26), with ζ and ξ that generally depend on the loading path and are different for normal and tangential components. The results for coordination number $\Gamma = 5.0$ are shown in Fig. 6 for the normal and tangential components of relative displacement and force. A fairly good agreement is found between actual and local adjustment fields, especially for the relative displacement.

More detailed results for the coefficients ζ for generalized uniform strain are presented by Kruyt and Rothenburg (2001).

6.3. Correlation function and length

The particle displacements are to a large extent determined by the imposed boundary displacements (prescribed strain). Hence the particle displacement U_i^p can be expressed as the sum of two terms, the regular displacement $\bar{U}_i^p = \varepsilon_{ij} X_j$ corresponding to uniform strain and a fluctuation u_i^p. Contrary to the regular displacement $\bar{U}_i^p$, this fluctuation will be independent of position for a statistically homogeneous assembly. Measures for the distance over which displacements of two particles are correlated are the *correlation function* $\rho_u(r)$ and *correlation length* L_u. For the fluctuation displacement u they are defined by the averages

$$\rho_u(r) = \frac{\overline{u(x)u(x+r)}}{\bar{u}^2}, \quad L_u = \int_0^\infty \rho_u(r)\,\mathrm{d}r, \tag{27}$$

with analogous definitions for the correlation function $\rho_\phi(r)$ and the correlation length L_ϕ of the force potential fluctuation. Note that for isotropic and statistically homogeneous assemblies under compressive loading, the right-hand side of Eq. (27) does not depend on position $\boldsymbol{x}$ and relative position $\boldsymbol{r}$, but only on the distance r between points.

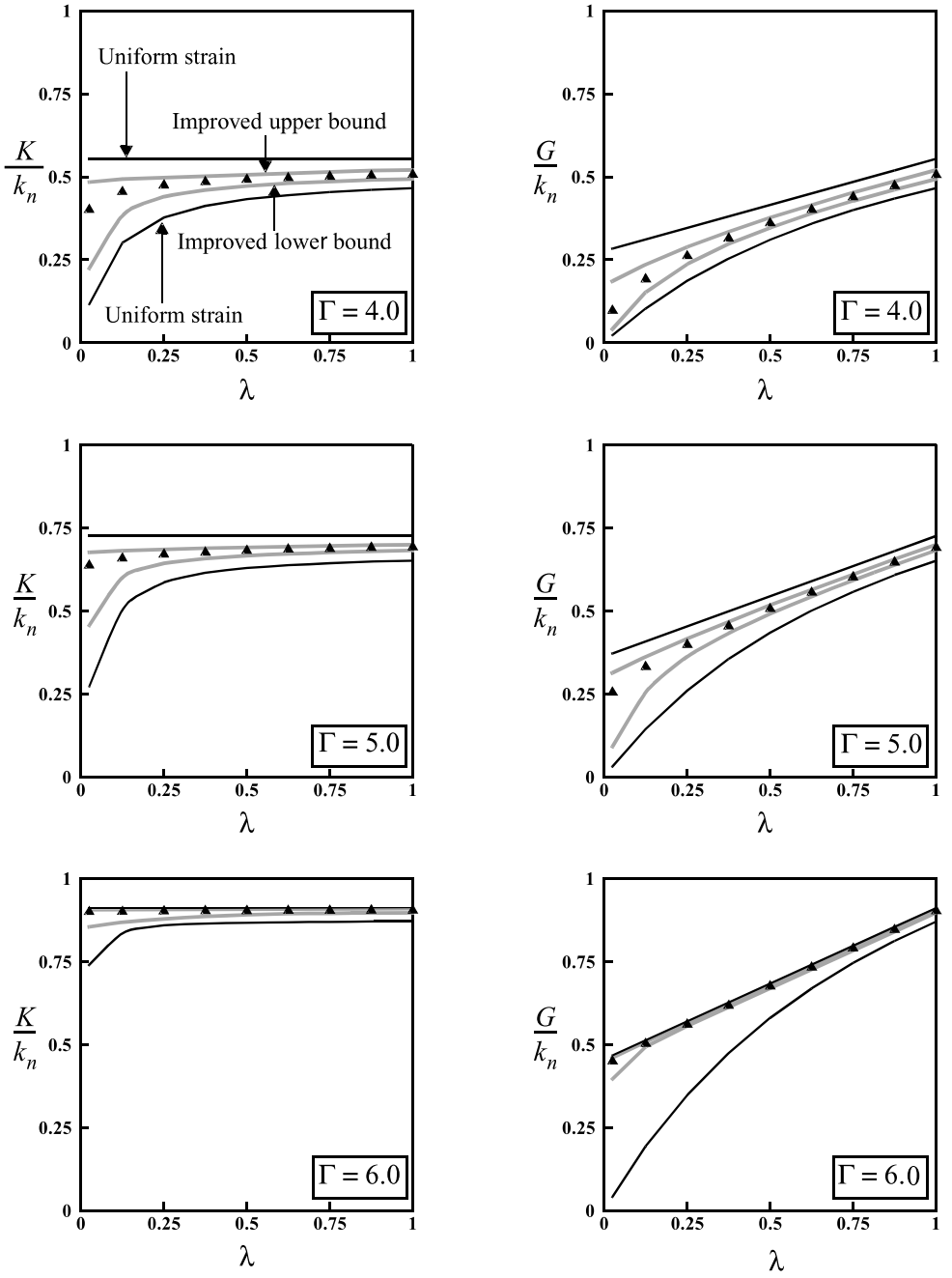

Fig. 5. Comparison of bounds with actual bulk modulus K and shear modulus G from discrete element simulations for various coordination numbers Γ and stiffness ratios λ; upper and lower line: uniform strain and uniform stress bounds; thick grey lines: improved bounds from local adjustment fields; triangles: actual moduli from discrete element simulations.

The correlation functions $\rho_u(r)$ and $\rho_\Phi(r)$ are shown in Fig. 7, as determined from the results of the discrete element simulations. Due to the finite particle size, no data are available for small distances, except

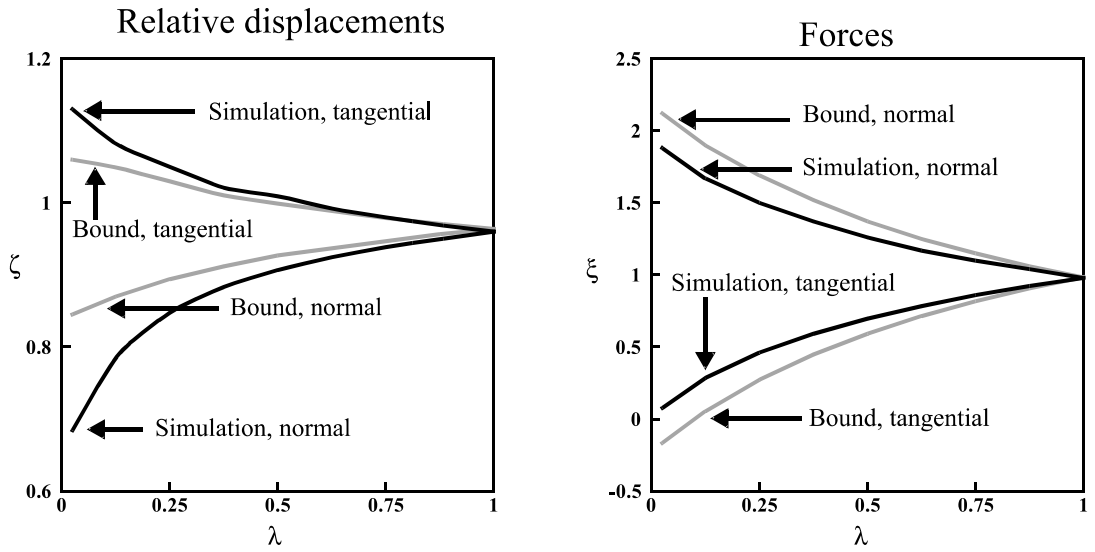

Fig. 6. Generalized uniform strain and stress: comparison of results from simulations and local adjustment bounds for coordination number $\Gamma = 5.0$ in shear for various stiffness ratios λ.

the trivial $\rho_u(0) = 1$ and $\rho_\phi(0) = 1$. Also shown in Fig. 7 is the natural logarithm of the correlation functions, which shows a linear behaviour for larger distances. This means that the correlation functions themselves exhibit an exponential decay. As expected for an isotropic assembly, correlation functions for both components of the displacement and force potential fluctuations were practically identical.

The computed correlation lengths are $L_u \cong 6R_{\text{avg}}$ and $L_\phi \cong 29R_{\text{avg}}$, where R_{avg} is the average particle radius. The size of the periodic box L_{box} is such that $L_{\text{box}} \cong 425R_{\text{avg}}$.

For properly conducted discrete element simulations where (periodic) *boundary effects* are negligible, we must have $L_{\text{box}}/2 \gg L_u$. Note that discrete element simulations are generally formulated in terms of displacements. This requirement can be reformulated into a lower bound for the required number of particles N

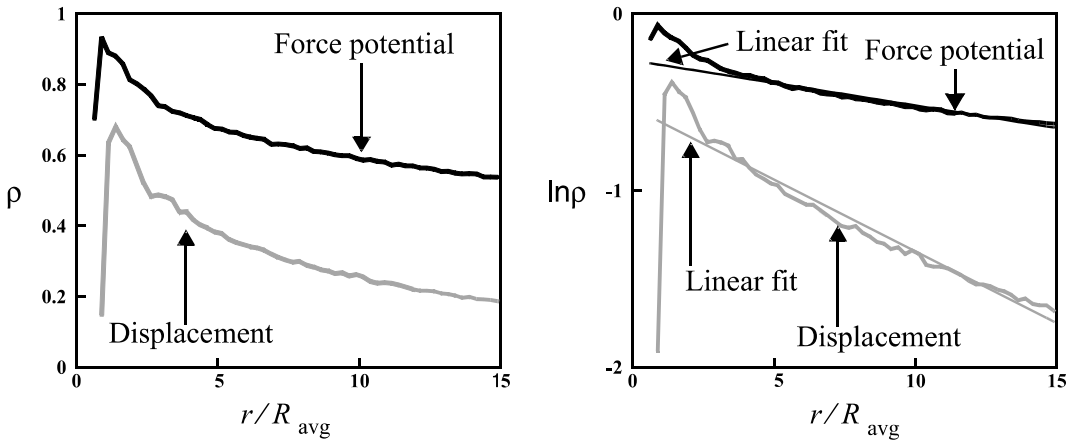

Fig. 7. Correlation functions ρ of displacement fluctuation and force potential fluctuation, as determined from the discrete element simulation for coordination number $\Gamma = 5.0$ and stiffness ratio $\lambda = 0.5$ in compression.

in simulations. For a periodic box of spatial dimension d ($d = 2$ or 3) with a square ($d = 2$) or cubic packing ($d = 3$) of the particles we have $N^{1/d}2R_{\text{avg}} \cong L_{\text{box}}$. With typical values of $L_u \cong 6R_{\text{avg}}$ and $L_{\text{box}}/2 \geqslant 5L_u$, we obtain the requirements $N \geqslant 900$ in two dimensions and $N \geqslant 27000$ in three dimensions (assuming that the correlation length in three dimensions is the same as that in two dimensions).

7. Discussion

A micromechanical study was made of the elastic behaviour of two-dimensional assemblies of non-rotating particles with bonded contacts. Based on the results of discrete element simulations, it was shown that the case of non-rotating particles is the limit case of couple stiffness $k_\omega \to \infty$. In the absence of body forces, the family of equilibrated contact forces is described, using force potentials (Satake, 1992). Applying minimum potential energy and minimum complementary energy principles, rigorous upper and lower bounds for the elastic moduli can be determined. Based on local adjustments to uniform fields, compatible displacement fields and equilibrated force potential fields are constructed that approximately satisfy equilibrium and compatibility, respectively. A comparison with the actual moduli, as determined from discrete element simulations, demonstrates that these bounds tightly bracket the moduli. More detailed analyses of the relative displacement and force fields at the contacts show that these match the actual fields fairly closely. The computed correlation length L_u is fairly small, while L_ϕ is larger. This indicates why the formulation based on displacements gives a more accurate prediction of the actual fields than the formulation based on force potentials (see Fig. 6).

The physical picture that emerges from this study is that the behaviour, either particle displacement or force potential, consists of two parts: (i) a regular part corresponding to a uniform field and (ii) a fluctuation part. The regular part is determined by the prescribed boundary conditions, while the fluctuation part is primarily determined by its *local environment*. This is corroborated by the fairly small correlation lengths, especially L_u. Whether this also holds for loose systems with particle rotation, contrary to the bonded systems without particle rotation that were studied here, has to be investigated. Results of photoelastic experiments (for example De Josselin de Jong and Verruijt, 1969; Drescher and De Josselin de Jong, 1972; Oda and Konishi, 1974) show that force chains are formed, which may be indicative of long range correlations. The condition $L_\phi > L_u$ observed here may be a *quantitative* indication of the presence of force chains.

The obtained bounds can be further improved by considering other fields for the displacement and force potential fields. This can be accomplished by adding more near-neighbours in the local adjustment analyses. Current research is dealing with the extension and application of the proposed procedure towards the more complex case *with* particle rotations.

References

Bathurst, R.J., Rothenburg, L., 1988. Micromechanical aspects of isotropic granular assemblies with linear contact interactions (Transactions of the ASME). Journal of Applied Mechanics 55, 17–23.

Chang, C.S., Liao, C.L., 1990. Constitutive relation for a particular medium with the effect of particle rotation. International Journal of Solids and Structures 26, 437–453.

Cundall, P.A., Strack, O.D.L., 1979. A discrete numerical model for granular assemblies. Géotechnique 9, 47–65.

De Josselin de Jong, G., Verruijt, A., 1969. Etude photo-élastique d'un empilement de disques. Cahier Groupe Français Rhéologie 2, 73–86.

Drescher, A., De Josselin de Jong, G., 1972. Photoelastic verification of a mechanical model for the flow of a granular materials. Journal of the Mechanics and Physics of Solids 20, 337–351.

Kruyt, N.P., Rothenburg, L., 1996. Micromechanical definition of the strain tensor for granular materials (Transactions of the ASME). Journal of Applied Mechanics 63, 706–711.

Kruyt, N.P., Rothenburg, L., 1998. Statistical theories for the elastic moduli of two-dimensional assemblies of granular materials. International Journal of Engineering Science 36, 1127–1142.

Kruyt, N.P., Rothenburg, L., 2001. Statistics of the elastic behaviour of granular materials. International Journal of Solids and Structures 38, 4879–4899.

Murdoch, J.B., 1970. Network theory. McGraw-Hill, New York, NY, USA.

Oda, M., Konishi, J., 1974. Microscopic deformation mechanism of granular material in simple shear. Soils and Foundations 14, 25–38.

Oda, M., Iwashita, K., 2000. Study on couple stress and shear band development in granular media based on numerical simulation analyses. International Journal of Engineering Science 38, 1713–1740.

Rothenburg, L., 1980. Micromechanics of idealised granular materials. PhD Thesis, Department of Civil Engineering, Carleton University, Ottawa, Ontario, Canada.

Satake, M., 1992. A discrete mechanical approach to granular materials. International Journal of Engineering Science 30, 1525–1533.

Washizu, K., 1968. Variational methods in elasticity and plasticity. Pergamon Press, Oxford, UK.